



VISTA INTERNATIONAL JOURNAL ON ENERGY, ENVIRONMENT & ENGINEERING



Effects of Al doping with zinc ferrite nanoparticles on structural, magnetic and dielectric properties

Sunanda Tambe¹ and R. Y. Borse²

¹Padmashri Vikhe Patil College of Art, Science and Commerce, Loni-Pravaranagar 413713, India (MS)

²Mahant Jamnadas Maharaj Arts, Commerce and Science College Karanjali, (Nashik).

*Corresponding author E-mail : talolesunanda@gmail.com Mob.: +91-9890451809.

ABSTRACT

Zinc ferrite nanoparticles have wide range of the applications in the field of Electronics, Optoelectronics, Magnetics, Solar cell, Photocatalysts. With Al doping we modify their structural, magnetic and electrical properties of zinc ferrite (ZnFe_2O_4). In the present studies, zinc ferrite nanoparticles were prepared by sol gel method using glycine as combustion agent. The effects of Al doping concentration on the structural, morphological, optical, magnetic and electrical properties of zinc ferrites were studied. In x-ray diffraction patterns analysis confirmed the formation of the cubic spinel structure. We characterise scanning electron microscopy (SEM) with energy dispersive X-ray (EDX) in the current work to examine the morphology of the nanomaterials. The UV-Vis optical investigation showed that Al^{+3} doping increased absorbance and significantly decreased energy band gap value (1.90 eV-2.01 eV). The magnetic properties of zinc ferrite NPs were studied by using vibrating samples magnetometer which showed samples of pure zinc ferrites and Al-doped zinc ferrite with paramagnetism. Dielectric properties were studied from impedance analyser. When aluminium concentration increases in the zinc ferrites, dielectric characteristic results were obtained in which dielectric constant (ϵ'), dielectric loss (ϵ'') and tangent loss decreased. Also when frequency increases above all three dielectric parameters remains stable at high frequency. The obtained results of pure and Al doped Zn ferrite are useful for high frequency applications.

Keywords : Zinc ferrite, Al doping, Sol-gel autocombustion, XRD, Dielectric constant.

1. Introduction:

In nanoscience field cubic spinel ferrite have (MFe_2O_4 , M = Zn, Mg, Co, Fe, Mn, Cu, and Ni) excellent magnetic properties due to their particle size and shape. Spinel ferrites nanoparticles are prepared with different method like Microemulsion, Ultrasonic (Sonochemical), non-hydrolytic, Sol-gel, Microwave-

Assisted, Mechanical Milling, solvothermal, electrochemical synthesis, Coprecipitation and Hydrothermal methods. Spinel ferrite nanoparticles have different shapes like cubic, spherical octahedral, or symmetric. All the prepared samples are annealed which results in improving their structural, magnetic and electrical properties.

- [1] Spinel ferrite nanoparticles having larger specific surface area that is why used as a catalyst. They are classified into heterogeneous and homogeneous. In catalyst its cost, recovery and reuse are the important factors in photodegradation and wastewater treatments
- [2] Proper choice of synthesis method and chemical composition defined its lattice structure with enhanced physical and chemical properties. Spinel ferrite behaves supermagnetic if crystalline size is below 20nm. In supermagnetism magnetic field appears random direction. Superparamagnetic iron oxide nanoparticles are classified into two categories i.e. small synthetic $\gamma\text{-Fe}_2\text{O}_3$ (maghemite) or Fe_3O_4 (magnetite) particles with its core range in between 10 nm and 100 nm in diameter. Transition metal ions such as copper, cobalt, nickel, and manganese are mixed with iron oxides behaviours superparamagnetic and included into superparamagnetic iron oxide nanoparticles. These are used in biomedical applications
- [3] Smaller crystalline size and larger surface area to enhanced their structural, magnetic, electronic, and optical properties of spinel ferrite nanoparticles. Crystalline size and shape are changed to vary their physical, magnetic and chemical properties
- [4] The cubic spinel ferrite nanoparticles are most important aspects of about magnetism with the parameters of crystal and magnetic structure. Magnetic performance of the spinel ferrite is classified into three level like atomic level, single particle level and mesoscopic level. All these levels are depending on preparation method of the nanoparticles
- [5] Sol gel method is very easy and its annealing temperature used for converting gel to ash is important aspect for the particle size. In spinel ferrite nanoparticles diameter of particles is determined with the help of transmission electron microscopy (TEM) which gives true particle size. With reference to information of nanoparticle dimension in spinel ferrite are the types of shapes

like spherical, cubic, octahedral, and symmetric star. Transmission electron microscopy gives the knowledge of on aggregation, chaining of particles, morphological specifics, thickness of disordered surface layer and defects. In spinel ferrite nanoparticles structural, electrical and magnetic properties varied with their material composition, synthesis methods and nanoparticles sizes. Fuel like citric acid, urea and glycine varies chemical reaction with their chemical compositions

[6] In this paper we focused on sol–gel auto-combustion method due to their simple process nanoparticles with its high purity, composition homogeneity and well crystalline size of the spinel ferrite nanoparticles.

2. Experimental details

The experimental details are given as follow :

2.1 Synthesis of $\text{ZnFe}_{2-x}\text{Al}_x\text{O}_4$ nanoparticles

In order to synthesize Al modified ZnFe_2O_4 analytical graded Zinc (II) nitrate hexahydrate ($\text{Zn}(\text{NO}_3)_2 \cdot 6\text{H}_2\text{O}$), Iron (III) nitrate nonahydrate ($\text{Fe}(\text{NO}_3)_3 \cdot 9\text{H}_2\text{O}$) and aluminium nitrate nanohydrate ($\text{Al}(\text{NO}_3)_3 \cdot 9\text{H}_2\text{O}$) with purity of 99.9% were used raw materials in this synthesis, as such without further purification. $\text{ZnFe}_{2-x}\text{Al}_x\text{O}_4$ with $x=0, 0.1, 0.2, 0.3, 0.4$ were prepared by sol–gel autocombustion method using glycine as the fuel. Initially all the chemicals are used with their stoichiometric ratio 1:3 was dissolved in 200 ml distilled water. Drop wise add ammonia for maintaining pH 7 (i.e. neutral). Final solution was continuously stirred on a magnetic hot plate for upto 3-4 hrs under the temperature 70–90°C obtained sol. Gradually sol was convert brown colour organic gel. After forming gel we given to heat treatment at 120°C-130°C to remove water content, decompose hydroxyl groups, and organic matter. Autocombustion start in certain period brown $\text{ZnFe}_{2-x}\text{Al}_x\text{O}_4$ powder was formed. The brown powder was grind in an agate mortar to make a fine and homogenous powder. Fine powder was annealed at 600°C for 5 hrs in air for better crystallization. Fig.1 shows a flowchart representation of the zinc ferrite nanopowder synthesis.

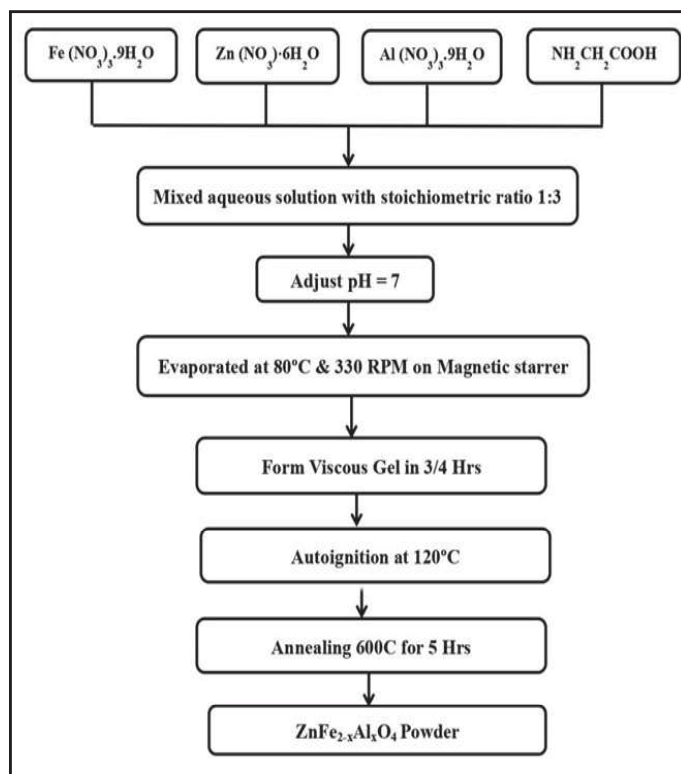


Fig.1 Flowchart of synthesis process preparing $\text{ZnFe}_{2-x}\text{Al}_x\text{O}_4$ sol gel autocombustion method

2.2. Characterization techniques

Crystal structure and phase composition of the prepared nanoparticle of the zinc ferrite was characterized by X-ray diffraction (XRD) analysis with $\text{CuK}\alpha$ radiation ($\lambda = 0.154 \text{ nm}$) within the angular range 20° - 80° . With the help of vibrating sample magnetometer (VSM) magnetic behaviour of the samples was studied. The dielectric properties of the nanoparticles including dielectric constant, real and complex permittivity, dielectric loss, and also AC conductivity with the help of LCR meter at broad frequency range were studied.

3 Result and discussion

3.1 Structural analysis

With X-ray diffraction (XRD) in the range of 2θ between 20° and 80° we investigated their structural analysis of the zinc ferrite nanoparticles. From the XRD patterns Fig.2 (a, b), it can be detected that all the reflection peaks of zinc ferrite and Al-doped zinc ferrite. The diffraction peaks at 2θ values of 29.85° , 35.2° , 36.83° , 42.8° , 53.11° , 56.61° , 62.16° , 70.51° , 73.52° and

74.57° correspond to major hkl planes (220), (311), (222), (400), (422), (511), (440), (620), (533) and (444) confirmed. All the diffraction peaks are corresponding that FCC structure with $\text{Fd}3\text{m}$ space group. We observed that there is no additional peak for both the samples. Higher diffraction peak at the (311) plane was considered as a measure of its better crystalline structure and phase purity [7, 8].

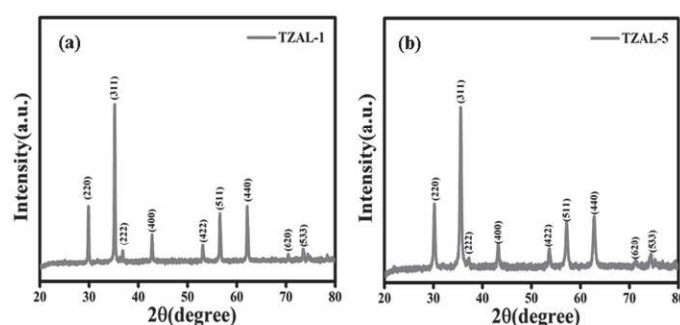


Fig.2.a XRD pattern of spinel ZnFe_2O_4 and b. X-ray diffraction Pattern of $\text{ZnFe}_{2-x}\text{Al}_x\text{O}_4$ (Al=0.4)

With the help of X-ray diffraction it can be observed that the width and the peaks changed due to deposition of aluminium ($x=0$ to 0.4) in $\text{ZnFe}_{2-x}\text{Al}_x\text{O}_4$ [9]. The crystallite size (D) of the spinel ferrite nanoparticles was calculated with the help of Debye-Scherrer's equation Eq. (1)

$$D = \frac{K\lambda}{\beta \cos \theta} \quad (1)$$

Where D is crystallite size, λ is the wavelength, θ is the Bragg's diffraction angle, β is the full width at half maximum (FWHM) and K is constant ($K=0.94$). The crystallite size was observed in the range 33-24 nm (Table 1). The crystallite size and lattice constant ' a ' decreased linearly with substitution of Al^{3+} in ZnFe_2O_4 . Lattice constant varies with the basis of difference in ionic radii, Al^{3+} ionic radius (0.051 nm) and Fe^{3+} (0.064 nm) of substituted ions [10]. Bond energy, synthesis method and chemical composition plays significant role to form crystalline size.

Table 1: Structural parameters of $\text{ZnFe}_{2-x}\text{Al}_x\text{O}_4$ ($x=0.0$ & 0.4)

Composition	Crystal structure	Lattice angle ($^\circ$)	Lattice parameter ($a = b = c$) ($^\circ$)	D (nm)	Volume (\AA^3)
ZnFe_2O_4	Cubic	$\alpha = \beta = \gamma = 90^\circ$	8.437	32.58	600.57
$\text{ZnFe}_{1.6}\text{Al}_{0.4}\text{O}_4$	Cubic	$\alpha = \beta = \gamma = 90^\circ$	8.359	24.15	584.07

3.2 Scanning Electron Microscopic (SEM) analysis

Scanning electron microscopy (SEM) was used to examine the appearance and structure of the produced material. Fig. 3 shows SEM images of unsubstituted and Al-substituted $\text{ZnFe}_{2-x}\text{Al}_x\text{O}_4$ spinel ferrite nanoparticles. The representative SEM profile images of $\text{ZnFe}_{2-x}\text{Al}_x\text{O}_4$ shown in Fig.3 (a & b) illustrates nanostructural behaviour of ferrite and doped ferrite samples. The ferrite samples of $\text{ZnFe}_{2-x}\text{Al}_x\text{O}_4$ where $x = 0.0, 0.3$ etc.

Table 2 (a) Elemental analysis of ZnFe_2O_4

Element	Weight %	Atomic %
O K	38.77	65.67
Fe K	42.32	25.61
Zn K	18.68	8.72
Total	100%	100%

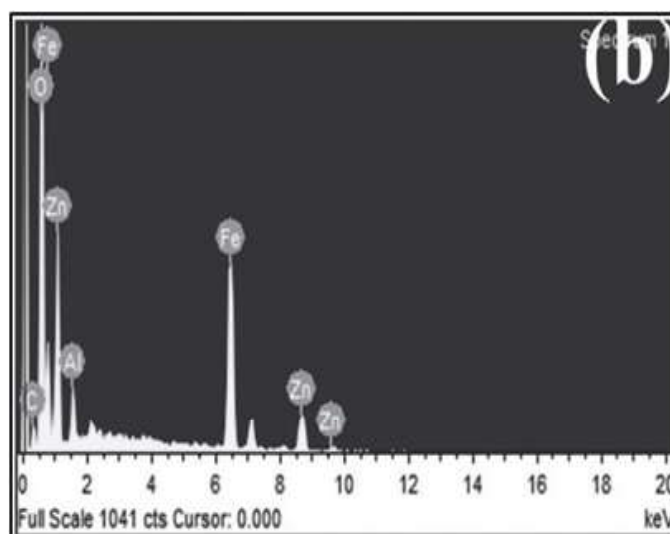
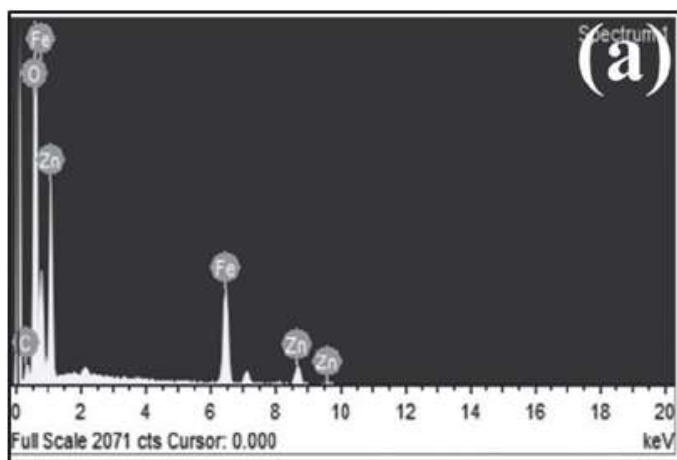
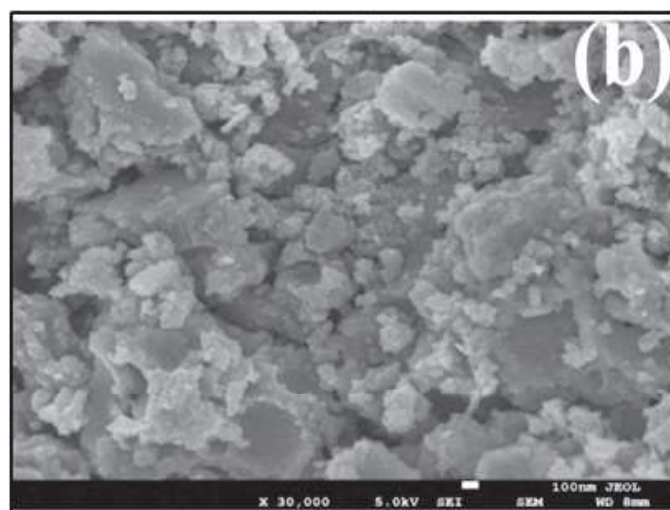
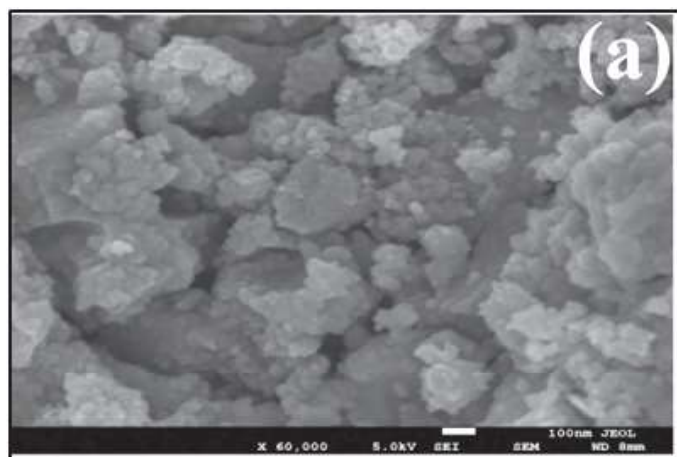
**Fig. 3 (a) SEM micrographs and EDX analysis of ZnFe_2O_4** **Fig. 3 (b) SEM micrographs and EDX analysis of $\text{ZnFe}_{1.7}\text{Al}_{0.3}\text{O}_4$**

Table 2 (b) Elemental analysis of ZnFe_{1.7}Al_{0.3}O₄

Element	Weight %	Atomic %
O K	42.67	64.26
Al K	8.55	5.77
Fe K	29.40	20.53
Zn K	19.38	9.44
Total	100%	100%

The incorporation of ions is said to change the particle size of the ferrite sample. As added Al³⁺ the crystalline grain size decreased. Al³⁺ substitution also had an impact on the sample's density, porosity, density, and lattice parameter [11].

3.3 Optical properties

UV-Visible absorption, reflectance, and transmittance analysis was used to evaluate the optical band gap and electrical architectures of the metal oxide semiconductor materials. In order to determine the band gap energy (E_g) of metal oxide semiconductors, UV-Visible diffuse reflectance spectroscopy (DRS) experiments are essential. The spinel ZnFe₂O₄ optical absorption characteristic, which is related to its electronic structural feature, is found to be a crucial determinant of the photocatalytic activity. The optical properties of the ZnFe_{2-x}Al_xO₄ (x= 0.0, 0.3) nanoparticles were investigated by UV-Vis spectroscopy. The absorbance of sample was measured in the wavelength range 200 nm –700 nm. The spinel ZnFe₂O₄ showed prolonged photoabsorption in this spectrum, extending from UV to visible area shorter than 750 nm, suggesting the prospect of strong photocatalytic activity of this material under visible light. The direct band gap energy of the specimen is determined from the Tauc plot by using Kubelka-Munk function. Fig.4 (a and b) shows the Tauc plot derived from absorbance spectra of the typical sample (ZnFe₂O₄). The band gap value determined from the Tauc plot was found to be 1.90 to 2.01 eV. ZnFe_{2-x}Al_xO₄ photoabsorption from the UV to visible area may be attributed to increased band gap energy levels brought on by the abundance of surface and interface defects in the aggregated nanoparticles

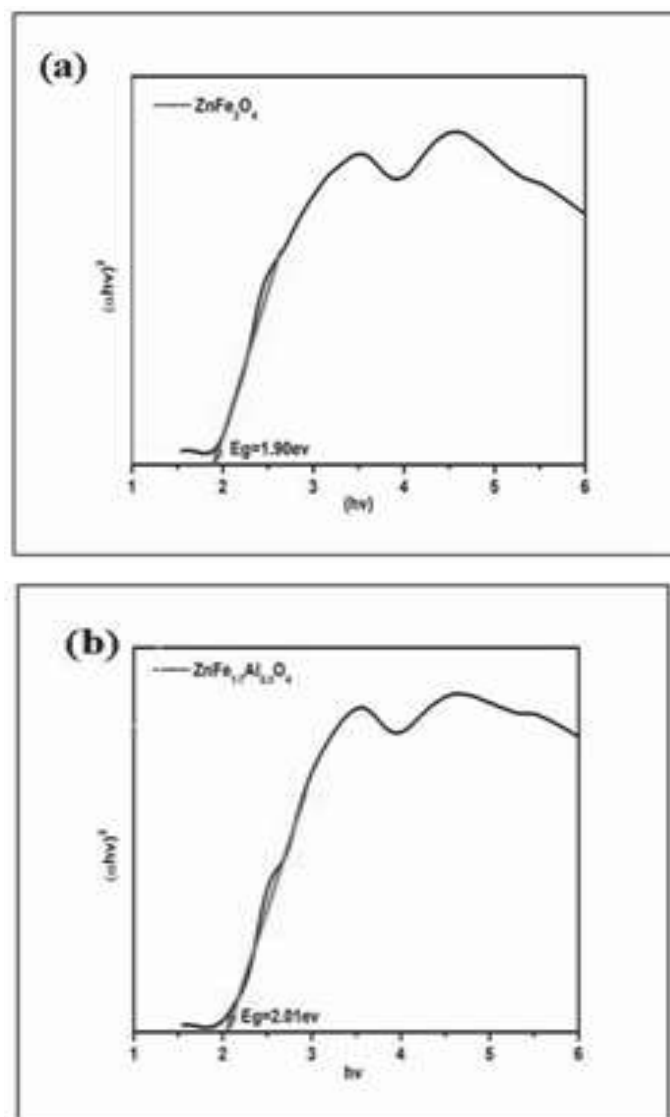


Fig.4. (a, b) UV-Vis plot of plot of nanoparticles ZnFe_{2-x}Al_xO₄(x=0.0, 0.3)

By analyzing UV-Visible absorption, reflectance, and transmittance data, the optical band gap and electrical structures of metal oxide semiconductor materials were identified. The following equation has been used to determine the band-gap energy with the use of Tauc plots.

$$\alpha h\nu = A(h\nu - E_g) \quad (2)$$

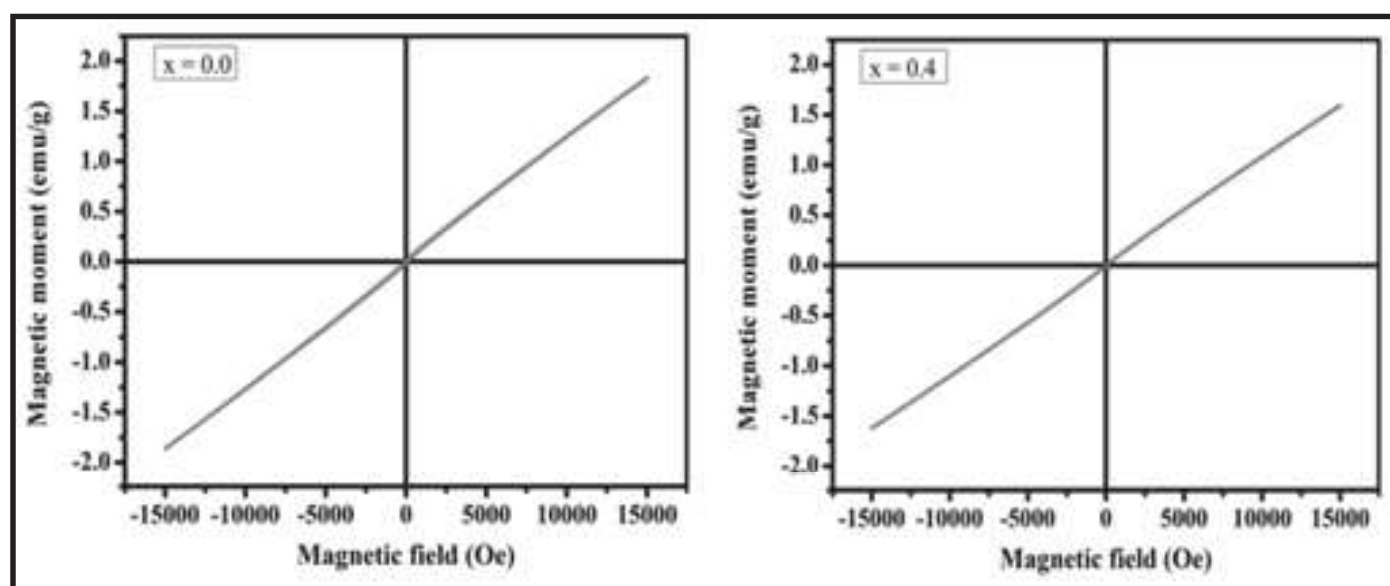
Where “A” is constant, “hν” is the photon energy ($\nu = c/\lambda$) “E_g” is the band gap energy of the material, and the exponent ‘n’ depends on the type of transition ($n = 1/2$ for direct allowed transition, $n = 2$ for indirect) [12].

Table 3 Band-gap energy of $\text{ZnFe}_{2-x}\text{Al}_x\text{O}_4$ ($x=0.0, 0.3$)

Sr.No	Composition	Band Gap(ev)
1.	ZnFe_2O_4	1.90
2.	$\text{ZnFe}_{1.7}\text{Al}_{0.3}\text{O}_4$	2.01

3.2 Vibrating sample magnetometry

With the help of vibrating-sample magnetometer (VSM) a magnetic property which is based on Faraday's Law of Induction was studied [13]. With the help of magnetic properties M-H curves of $\text{ZnFe}_{2-x}\text{Al}_x\text{O}_4$ nanoparticles was obtained. By analysis of M-H curves, we get the value of magnetic moment (μ), saturation magnetization (MS), remanence (Mr), coercivity (Hc) and the anisotropy constant (K) [14]. Magnetization totally depends on crystalline particle size, we observed magnetization decreases when particle size increases. Zinc ferrite nanoparticles behave ferromagnetic when particles size is 19-21nm and also paramagnetic behaviour when particle size 29 to 35nm [15].

**Fig. 5. Hysteresis loops of $\text{ZnFe}_{2-x}\text{Al}_x\text{O}_4$ nanoparticles**

The M-H curves of the magnetization in Fig.4 confirmed the paramagnetic behaviour of the nanoparticles. In plot magnetic field at x-axis and magnetization at y-axis data showed. In table 2 shows that values of magnetic parameters $\text{ZnFe}_{2-x}\text{Al}_x\text{O}_4$. In this case saturation magnetization decreases and aluminium composition increases and also due to smaller particle size as well as replacement of ions (Fe^{3+} to Al^{3+}). Mr (remanence) and Hc (coercivity) values were small due to their different bond energy of $\text{Al}^{3+}-\text{O}^{2-}$, $\text{Fe}^{3+}-\text{O}^{2-}$ and $\text{Zn}^{2+}-\text{O}^{2-}$ [16,17].

Table 3 The magnetic parameters of $\text{ZnFe}_{2-x}\text{Al}_x\text{O}_4$ nanoparticles

Composition	Ms (emu/g)	Mr (emu/g)	Hc (Oe)	Magnetic moment (μ)	Anisotropy constant
ZnFe_2O_4	1.832	0.0095	2.439	0.079	2.234
$\text{ZnFe}_{1.6}\text{Al}_{0.4}\text{O}_4$	1.601	0.0125	2.538	0.066	2.032

The magnetic moment of the $\text{ZnFe}_{2-x}\text{Al}_x\text{O}_4$ nanoparticles were calculated by the given formula.

$$\mu = \frac{MXM_s}{5585} \quad (3)$$

From Eq. (2) M = molecular mass of the material, M_s = saturation magnetization and also anisotropy constant of the synthesized $\text{ZnFe}_{2-x}\text{Al}_x\text{O}_4$ nanoparticles was calculated by the formula.

$$K = \frac{H_c XM_s}{2} \quad (4)$$

We observed small value of the coercivity for benefits to use as a soft magnetic materials and low resistive for magnetization. Substitution of aluminum in spinel ferrite (Ni–Zn ferrite) is not found in literature in bulk due to their saturation magnetization (M_s), and magnetic moment (μ) decrease. Finally we got the result increased substitution of aluminium decreased its magnetic moment (μ), this effect is known to spin canting [18].

3.3 Frequency dependent dielectric property

Dielectric properties totally depend upon the type of ferrite, doping concentration, annealing temperature and it's time, synthesis method, structural parameters, crystalline size, porosity, density and polymer which are used in composite sample [19]. Complex permittivity in dielectric study can be expressed by the relations in Eq (4).

$$\epsilon = \epsilon' + i\epsilon'' \quad (5)$$

Where, ϵ' is the real part and ϵ'' imaginary parts of dielectric constant. Electric permittivity high values are occurs from thin grain boundary [20]. Dielectric properties were analysed using Maxwell-Wagner model, Koop's phenomenological theory. We use Koop's theory to establish frequency and AC conductivity relations in different ferrites. In the

dielectric properties of $\text{ZnFe}_{2-x}\text{Al}_x\text{O}_4$ dielectric constant, complex permittivity, dielectric loss, and AC conductivity with the help of LCR meter can be calculated [21, 22]. This mentioned parameters are very important for the application of high frequency. Zinc ferrite is referred as soft magnetic material due to their low coercivity, magnetization which can be easily reversible [23]. The dielectric constant (ϵ') of the pellet can be calculated by using the formula

$$\epsilon' = \frac{C_p X t}{\epsilon_0 X A} \quad (6)$$

Where, ϵ_0 is permittivity of the free space, C_p is capacitance of pellet, t is thickness of the pellet, and A is area of the pellet. Dielectric loss tangent or dissipation of the dielectric ($\tan\delta$) can be calculated by using the formula

$$\tan \delta = \frac{1}{Q} \quad (7)$$

Dielectric loss tangent is simply reciprocal of quality factor Q and the dielectric loss (ϵ'') of the material is,

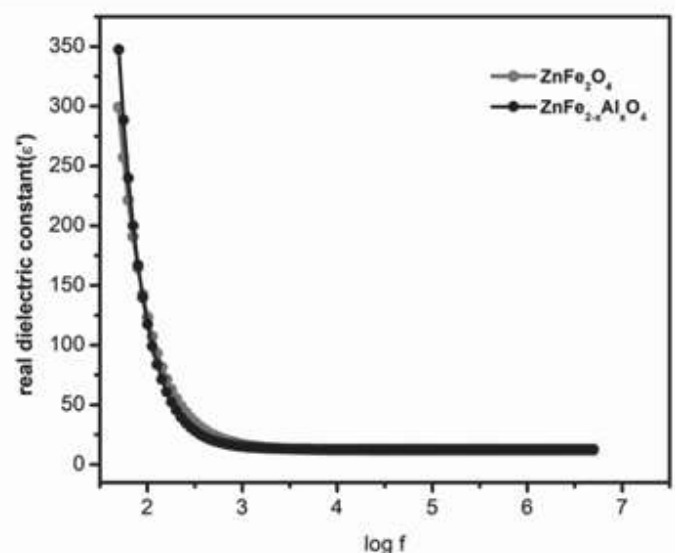


Fig. 6a. Real dielectric constant of $\text{ZnFe}_{2-x}\text{Al}_x\text{O}_4$ ($x=0.0\&0.4$) with frequency

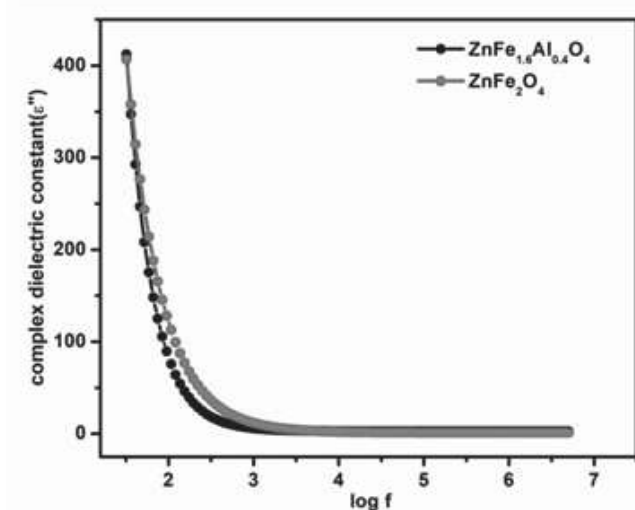


Fig. 6b. Complex dielectric constant of $\text{ZnFe}_{2-x}\text{Al}_x\text{O}_4$ ($x=0.0\&0.4$) with frequency

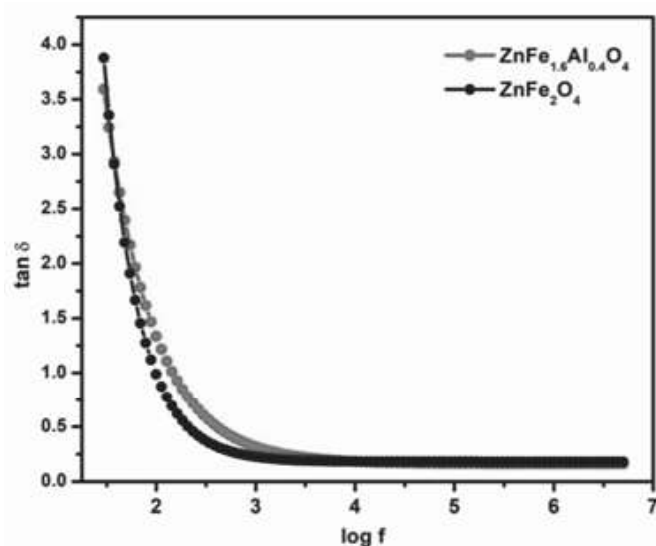


Fig. 6c. Loss tangent of $\text{ZnFe}_{2-x}\text{Al}_x\text{O}_4$ ($x=0.0\&0.4$) with frequency

Composition	At 50Hz			At 5KHz		
	ϵ'	ϵ''	$\tan \delta$	ϵ'	ϵ''	$\tan \delta$
ZnFe_2O_4	306.03	197.49	0.68	13.22	4.29	0.30
$\text{ZnFe}_{1.6}\text{Al}_{0.4}\text{O}_4$	342.07	414.06	3.40	12.66	4.71	0.18

Fig. 6(a to c) depicts the relationship between frequency and real dielectric constant(ϵ'), complex dielectric constant(ϵ'') and Loss tangent($\tan\delta$) for $\text{ZnFe}_{2-x}\text{Al}_x\text{O}_4$ nanoparticles produced using the sol-gel

auto-combustion technique with glycine as an fuel agent and 600°C. The value of ϵ' and ϵ'' is high at low frequencies, as can be shown in mentioned fig of 4a and 4b eventually falls off as the when frequency rises. The free charge mobility within the material is what causes the high value of ϵ'' at low frequency. The contributions of electronic, ionic, orientation, and interfacial polarisation determine the characteristics of ϵ' and ϵ'' at low frequencies [24]. All the parameters like dielectric constant (real and complex) and dielectric loss for all the samples were studied in the frequency range 50Hz-5MHz. All the parameters are frequency dependent. It values mostly depends on the chemical composition, fabrication route, crystallite size and cation distribution [25]. In all the compositions of sample of $\text{ZnFe}_{2-x}\text{Al}_x\text{O}_4$ if frequency is increases dielectric parameters are decreases. According to Koop's model $\tan \delta$ values varied with their frequency range due to their energy loss of Fe^{2+} and Fe^{3+} . Basically at high very frequency resistivity and grains plays vital role and for hopping of electrons in between Fe^{2+} and Fe^{3+} need energy and $\tan \delta$ is very small [26,27,28].

4 Conclusions

Nanocrystalline $\text{ZnFe}_{2-x}\text{Al}_x\text{O}_4$ ($x=0.0, 0.1, 0.2, 0.3, 0.4$) nanoparticles were successfully prepared with sol gel autocombustion method with glycine as a fuel. Sol gel method was preferred because of low cost, good crystallinity and reproducibility. Crystalline size was found to vary within range of 32 to 24nm. XRD showed that the formations of cubic face centred structure are confirmed. Al content was added lattice parameters 8.437 to 8.359 reduced. VSM show paramagnetic behaviour due to their particle size 29 to 35nm. The dielectric constant and dielectric loss both are decreased at high frequency.

Acknowledgments

The authors are grateful to Dr. K.M. Jadhav, Department of Physics, Dr. Babasaheb Ambedkar Marathwada University, Aurangabad.

References :

- [1] Pacakova, B., Kubickova, S., Reznickova, A., Niznansky, D., & Vejpravova, J. (2017). Spinel ferrite nanoparticles: correlation of structure and magnetism. *Magnetic Spinel—Synthesis, Properties and Applications*, 4-6.
- [2] Kefeni, K. K., & Mamba, B. B. (2020). Photocatalytic application of spinel ferrite nanoparticles and nanocomposites in wastewater treatment. *Sustainable materials and technologies*, 23.
- [3] Arora, S. (2012). Superparamagnetic iron oxide nanoparticles: magnetic Nano platforms as drug carriers. *International journal of nanomedicine*, 7, 3445.
- [4] Tatarchuk, T., Bououdina, M., Judith Vijaya, J., & John Kennedy, L. (2016, August). Spinel ferrite nanoparticles: synthesis, crystal structure, properties, and perspective applications. In *International conference on nanotechnology and nanomaterials* (pp. 305-325). Springer, Cham.
- [5] López-Ortega, A., Lottini, E., Fernandez, C. D. J., & Sangregorio, C. (2015). Exploring the magnetic properties of cobalt-ferrite nanoparticles for the development of a rare-earth-free permanent magnet. *Chemistry of materials*, 27(11), 4048-4056.
- [6] Lwin, N., Othman, R., Sreekantan, S., & Fauzi, M. A. (2015). Study on the structural and electromagnetic properties of Tm-substituted Mg–Mn ferrites by a solution combustion method. *Journal of Magnetism and Magnetic Materials*, 385, 433-440.
- [7] Mund, H. S., & Ahuja, B. L. (2017). Structural and magnetic properties of Mg doped cobalt ferrite nano particles prepared by sol-gel method. *Materials Research Bulletin*, 85, 228-233.
- [8] Joshi, S., Kumar, M., Chhoker, S., Kumar, A., & Singh, M. (2017). Effect of Gd³⁺ substitution on structural, magnetic, dielectric and optical properties of nanocrystalline CoFe₂O₄. *Journal of Magnetism and Magnetic Materials*, 426, 252-263.
- [9] Cheema, H., Yadav, V., Maurya, R. S., Yadav, V., Kumar, A., Sharma, N., ...& Kumar, U. (2021). Structural, optical and electrical properties of Mn-doped ZnFe₂O₄ synthesized using sol–gel method. *Journal of Materials Science: Materials in Electronics*, 32(18), 23578-23600.
- [10] Mahmood, M., Yousuf, M. A., Baig, M. M., Imran, M., Suleman, M., Shahid, M., & Warsi, M. F. (2018). Spinel ferrite magnetic nanostructures at the surface of graphene sheets for visible light photocatalysis applications. *Physica B: Condensed Matter*, 550, 317-323.
- [11] Ullah Rather, S., & Lemine, O. M. (2020). Effect of Al doping in zinc ferrite nanoparticles and their structural and magnetic properties. *Journal of Alloys and Compounds*, 812, 152058.
- [12] Jadhav, S. A., Khedkar, M. V., Andhare, D. D., Gopale, S. B., & Jadhav, K. M. (2021). Visible light photocatalytic activity of magnetically diluted Ni–Zn spinel ferrite for active degradation of rhodamine B. *Ceramics International*, 47(10), 13980-13993.
- [13] Gul, S., Yousuf, M. A., Anwar, A., Warsi, M. F., Agboola, P. O., Shakir, I., & Shahid, M. (2020). Al-substituted zinc spinel ferrite nanoparticles: Preparation and evaluation of structural, electrical, magnetic and photocatalytic properties. *Ceramics International*, 46(9), 14195-14205.
- [14] Kirupakar, B. R., Vishwanath, B. A., & Sree, M. P. (2016). Vibrating sample magnetometer and its application in characterisation of magnetic property of the anticancer drug magnetic microspheres. *International Journal of Pharmaceutics and Drug Analysis*, 227-233.
- [15] Yousuf, M. A., Jabeen, S., Shahi, M. N., Khan, M. A., Shakir, I., & Warsi, M. F. (2020). Magnetic and electrical properties of yttrium substituted manganese ferrite nanoparticles prepared via micro-emulsion route. *Results in Physics*, 16,

- 102973.
- [16] Anjaneyulu, T., Raghavender, A. T., Kumar, K. V., Murthy, P. N., & Narendra, K. (2014). Effect of particle size on the structural and magnetic properties of nanocrystalline zinc ferrite. *Science, Technology and Arts Research Journal*, 3(3), 48-51.
- [17] Giri, M. S., Sahu, D. K., Sarkar, N. N., & Rewatkar, K. G. Influence of Aluminium ion substitution on Structural and Magnetic Properties of nano-structured BaFe₁₂O₁₉ Powder.
- [18] Wahba, A. M., Ali, N. A., & Eltabey, M. M. (2014). Effect of Al-ion substitution on structural and magnetic properties of Co–Ni ferrites nanoparticles prepared via citrate precursor method. *Materials Chemistry and Physics*, 146(3), 224-229.
- [19] Raghavender, A. T., Pajic, D., Zadro, K., Milekovic, T., Rao, P. V., Jadhav, K. M., & Ravinder, D. (2007). Synthesis and magnetic properties of NiFe_{2-x}Al_xO₄ nanoparticles. *Journal of Magnetism and Magnetic Materials*, 316(1), 1-7.
- [20] Lumbantoruan, M. A., & Suharyadi, E. (2020). Effect of Zn on Dielectric Properties of Co-ZnFe₂O₄ Magnetic Nanoparticles. In *Key Engineering Materials* (Vol. 840, pp. 448-453). Trans Tech Publications Ltd.
- [21] Adnan, M., Usman, M., Akram, M. A., Javed, S., Ali, S., Ahmad, I., & Islam, M. (2021). Study of magnetic and dielectric properties of ZnFe₂O₄/CoCr₂O₄ nanocomposites produced using sol-gel and hydrothermal processes. *Journal of Alloys and Compounds*, 865, 158953.
- [22] Baba-Ahmed, I., Gherca, D., Iordan, A. R., Palamaru, M. N., Mita, C., Baghdad, R., & Abderrahmane, A. (2021). Sequential Synthesis Methodology Yielding Well-Defined Porous 75% SrTiO₃/25% NiFe₂O₄ Nanocomposite. *Nanomaterials* 2022, 12, 138.
- [23] Andhare, D. D., Patade, S. R., Jadhav, S. A., Somvanshi, S. B., & Jadhav, K. M. (2021). Rietveld refined structural, morphological, Raman and magnetic investigations of superparamagnetic Zn–Co nanospinel ferrites prepared by cost-effective co-precipitation route. *Applied Physics A*, 127(6), 1-13.
- [24] Yadav, R. S., Havlica, J., Masilko, J., Tkacz, J., Kuřitka, I., & Vilcakova, J. (2016). Anneal-tuned structural, dielectric and electrical properties of ZnFe₂O₄ nanoparticles synthesized by starch-assisted sol–gel auto-combustion method. *Journal of Materials Science: Materials in Electronics*, 27(6), 5992-6002.
- [25] Ghodake, J. S. (2018). Dielectric Behavior of Dysprosium Substituted Magnesium Ferrite. *Material Science Research India* (Online), 15(1), 48-54.
- [26] Khan, M. A., Sabir, M., Mahmood, A., Asghar, M., Mahmood, K., Khan, M. A., ... & Warsi, M. F. (2014). High frequency dielectric response and magnetic studies of Zn_{1-x}Tb_xFe₂O₄ nanocrystalline ferrites synthesized via micro-emulsion technique. *Journal of magnetism and magnetic materials*, 360, 188-192.
- [27] Zeljka, C., Srđan, R., Jankov, S., Sonja, S., & Agneš, K. (2009). Dielectric properties and conductivity of zinc ferrite and zinc ferrite doped with yttrium. *Journal of Alloys and Compounds*.
- [28] Saqib, H., Rahman, S., Susilo, R., Chen, B., & Dai, N. (2019). Structural, vibrational, electrical, and magnetic properties of mixed spinel ferrites Mg_{1-x}Zn_xFe₂O₄ nanoparticles prepared by co-precipitation. *AIP Advances*, 9(5), 055306.